Nucleation of Ice in Confined Geometry

J. M. Baker and J. C. Dore*

Physics Laboratory, University of Kent, Canterbury, Kent, CT2 7NR, U.K.

P. Behrens

Institut für Anorganische Chemie, Ludwig Maximilians Universität, München, Germany

Received: October 11, 1996; In Final Form: February 27, 1997[⊗]

Neutron diffraction studies have been made of ice nucleation in various forms of porous sol−gel silicas and ordered aluminosilicates. It is shown that the crystal structure of the ice exhibits significant variation according to the conditions and often has a diffraction pattern composed of a hybrid with both cubic and hexagonal ice characteristics. The ice structures appear defective/disordered in a complex manner but have common characteristics in terms of temperature variation studies. New studies of water in ordered mesoscopic (MCM-41) structures give results that appear to indicate "frustrated nucleation".

1. Introduction

It is well-known that the freezing point of a liquid in the confined geometry of a solid porous matrix is depressed below the normal freezing point of the bulk phase liquid. In the case of water the resulting ice phase can have quite different characteristics from the hexagonal ice Ih formed under normal conditions. Neutron diffraction studies[1,2] of ice nucleation in a sol−gel silica with a pore size of ∼90 Å showed a depression of ∼17 °C and the creation of a crystalline ice with structure similar to that of metastable cubic ice, Ic. Subsequent studies[3] have confirmed this general behavior but have also emphasized that the detailed features are strongly influenced by pore size, pore shape, filling factor, and thermal history.

The present paper provides a short review of recent neutron diffraction studies of ice nucleation in a range of silica samples under differing conditions. The observations demonstrate that the phase transition and subsequent crystal growth are quite complex and the resulting crystal structures appear as a hybrid with cubic and hexagonal characteristics. In other cases, the nucleation/growth process seems to be completely suppressed, and the diffraction pattern does not exhibit any sharp Bragg peaks. The study of ice in confined geometry can therefore provide a rich source of information on phase stability, defective/disordered states, and hydrogen-bonded networks for a range of reproducible ice systems.

2. Theoretical Framework

Studies of liquids in confined geometry by neutron diffraction have developed over two decades, but it is comparatively recently that detailed studies have been made of nucleation processes using this technique. There are two basic approaches based on the direct evaluation of the crystallographic pattern or the use of difference function methods to compare the solid and liquid phases. The theoretical framework for neutron diffraction studies has been presented elsewhere,[4] and only a brief review of the main formalism will be presented here.

Most studies have been made of water/ice in porous silicas due to the high pore volume and availability of samples with different characteristics. The diffraction measurements are made for the dry sample material and also for the sample containing the liquid or nucleated solid under investigation. The scattering pattern for a water/ice sample can then be evaluated by a simple subtraction:

$$I_W(Q) = I_{W+S}(Q) - f_S I_S(Q) \quad (1)$$

where $I(Q)$ represents the intensity as a function of the scattering vector, Q, with subscripts for water (W) and substrate (S), and incorporates a self-attenuation correction factor f_S, which is close to unity. The function $I_W(Q)$ represents, to a good approximation, the diffraction pattern for confined water/ice and can be used to determine the molecular structure factor, $S_M(Q)$. For the bulk liquid, it is possible to decompose this function into contributions from individual molecules (intramolecular correlations) and the arrangement of molecules (intermolecular correlations) by writing

$$S_M(Q) = f_1(Q) + D_M(Q) \quad (2)$$

where $f_1(Q)$ is the molecular form factor and $D_M(Q)$ represents the liquid structure. The molecular form factor is an oscillatory function that dominates the high-Q region of the scattering distribution and for heavy water (D_2O) is given by

$$f_1(Q) = \frac{1}{(b_O + 2b_D)^2}[b_O^2 + 2b_D^2 + 4b_O b_D j_0(Qr_{OD})_{exp}(-\gamma_{OD}Q^2) + 2b_D^2 j_0(Qr_{DD})_{exp}(-\gamma_{DD}Q^2)] \quad (3)$$

Here b denotes the atomic scattering length, $j_0(x) = \sin x/x$, $\gamma_{OD} = {}^1/_2\langle u_{OD}^2\rangle$, where $\langle u_{OD}^2\rangle$ is the mean square amplitude of displacement of the O and D atoms from equilibrium position due to the normal mode vibration of the molecule. The intermolecular spatial correlations in real space can be evaluated from the Fourier−Bessel transform,

$$d_L(r) = 4\pi\rho_M r[\bar{g}_L(r) - 1] = \frac{2}{\pi}\int_0^\infty QD_M(Q)\sin Qr\, dQ \quad (4)$$

where ρ_M is the molecular number density and $\bar{g}(r)$ is a composite pair correlation function. The r-space resolution, Δr, is inversely proportional to Q_{max} and is typically 0.3 Å for a reactor measurement. The finite size of the dispersed volume also leads to diffraction broadening in the measured profile, but this is a minor effect on the liquid structure factor.[1,2]

[⊗] Abstract published in *Advance ACS Abstracts,* June 1, 1997.

S1089-5647(96)03155-0 CCC: $14.00

TABLE 1: Characteristic Properties of the Porous Samples (The Pore Volumes of the MCM-41 Samples Are Not Known Accurately)

manufacturer	type	nominal pore width (Å)	pore volume (cm^3/g)	filling factor
Unilever	sol−gel	500	1.3	0.15
Unilever	sol−gel	200	1.71	0.36
Aldrich	sol−gel	60	0.75	1.0
Aldrich	sol−gel	40	0.44	1.0
Behrens	MCM-41	35	∼0.5	∼0.3
Behrens	MCM-41	33	∼0.5	∼0.3

If the liquid in the pores freezes to give a perfect crystalline solid, the intensity profile develops sharp Bragg peaks and is conventionally written as the crystal structure factor, $S(hkl)$, where h, k, and l are the Miller indices corresponding to different crystallographic planes. The size and shape of the randomly oriented crystallites affect the width of the diffraction peaks, which are symmetrically broadened in proportion to the inverse of the overall crystallite dimension. In addition, it is likely that the effects of the confining walls will introduce defects and disorder into the structure so that the diffraction pattern will also contain a diffuse scattering component that appears as a broad oscillatory function under the peaks, in a fashion similar to that of plastic crystals.[5] The predominant effect will clearly depend on the particular characteristics of the materials being studied.

A sensitive way of investigating structural change with temperature is to use the first-order difference method by writing

$$\Delta S_M(Q,T) = S_M(Q,T) - S_M(Q,T_0) = \Delta D_M(Q,T) \quad (5)$$

where T is the sample temperature and T_0 is a reference temperature; this procedure has the advantage of eliminating various experimental and analytic correction terms and yields directly the change in intermolecular correlations if the molecular conformation remains unchanged. The change in spatial characteristics $\Delta d_L(r,T)$ can also be evaluated by the analogue of eq 4, i.e.

$$\Delta d_L(r,T) = \frac{2}{\pi}\int_0^\infty Q\Delta D_M(Q,T) \sin Qr \, dQ \quad (6)$$

Water in the bulk and confined phase is found to exhibit significant structural change for relatively small temperature variations and has been fully studied.[6] The use of the difference function technique for phase transitions was first reported by Motl, Dore, and Bellissent-Funel[3,7] for partially filled sol−gel silicas and is again used for the treatment of the present data sets. The method is particularly useful in the present studies because it also eliminates the scattering from the substrate material.

3. Sample Preparation and Experimental Measurements

The nucleation of water was studied in two different pore morphologies using two neutron diffractometers −7C2 and G61—at the Orphée reactor, Laboratoire Léon Brillouin, CEN-Saclay, France. The 7C2 spectrometer uses neutrons of wavelength 0.7 Å; diffracted neutrons are detected by a position sensitive multidetector spanning 128° and gives an accessible Q-range of 0.5−16 $Å^{-1}$. The G61 instrument uses longer wavelength neutrons of 4.7 Å and provides higher Q-resolution data over a smaller range ($0.1 < Q < 2.5$ $Å^{-1}$) which is sufficient to encompass the main diffraction peaks in both cubic and hexagonal ice.

Table 1 lists the characteristics of the two types of porous materials used in this study, i.e. sol−gel silicas and MCM-41 type mesoporous aluminosilicates. The sol−gel silicas have a disordered pore structure with a well-defined mean radius, and the MCM-41 aluminosilicates consist of ordered, uniform mesopores. The pore structure of MCM-41 materials is reminiscent of a honeycomb, as they have a regular, hexagonal array of uniaxial channels.[8] The aluminosilicate samples both have similar pore widths (∼34 Å) and wall thicknesses (8 Å), but due to a different ratio of silicon to aluminum, the RJ31 sample is more hydrophilic ($AlSi_{24}O_{47}(OH)_6$) than the Al13 sample ($AlSi_{17}O_{34}(OH)_4$).

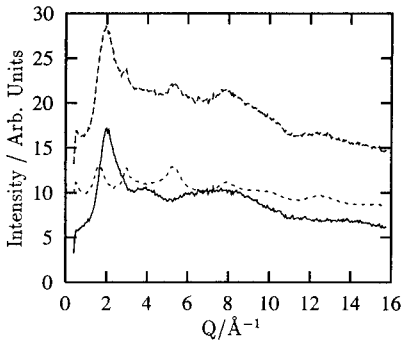

Figure 1. Diffraction pattern from D_2O fully filling Aldrich 60 Å silica at 25 °C. This pattern was obtained from subtracting the dry silica pattern (lower broken line) from the wet silica pattern (upper broken line).

Due to the large incoherent scattering length of hydrogen, D_2O is generally preferred to H_2O for neutron diffraction experiments on water. Therefore the porous materials, which are hygroscopic, require treatment to remove H atoms prior to use. Typically this involves drying at ∼120 °C for 10 h to remove any residual H_2O from the pores, followed by saturation with D_2O to ensure that any exchangeable hydrogen atoms in hydroxyl groups in the silica matrix are replaced by deuterons. After this has equilibrated (after, say, 5 h) the sample is dried again, in either a D_2O rich atmosphere or vacuum, prior to filling with the required amount of D_2O. The amount of water added to the dry substrate is described by the filling factor, f, which is defined as the ratio of water volume to the available pore volume. Table 1 gives the values of f for the samples studied here.

4. Results

4.1. Sol−Gel Silicas. The results for measurements of D_2O water in a sol−gel silica with 60 Å pore size are shown in Figure 1. The curves give the diffraction pattern for the "wet" and "dry" samples, showing the relative contribution from the water and silica; the resulting pattern for the confined water is also shown.

The full diffraction patterns for ice nucleation with variable filling factors for three different silica samples (see Table 1) are shown in Figure 2. It is immediately apparent that the first peak in the diffraction pattern (at ∼1.7 $Å^{-1}$) has a different form for the three samples. The ice formed in the partially full 500 Å pores has a clear triple peak corresponding to ice Ih, whereas the pattern from ice fully filling 40 Å pores has a single main peak (and higher order peaks) corresponding to a predominantly ice Ic phase. This behavior is more clearly defined in the higher resolution studies (shown as in the inset to Figure 2), which give a better definition of the peak profiles. The data for the 40 Å pores have a main central peak at 1.71 $Å^{-1}$, as expected for cubic ice, but also retain some subsidiary features of the hexagonal ice pattern with a distinctive asymmetric profile. The results for the 200 Å sample exhibit characteristics that are intermediate in form but still indicative

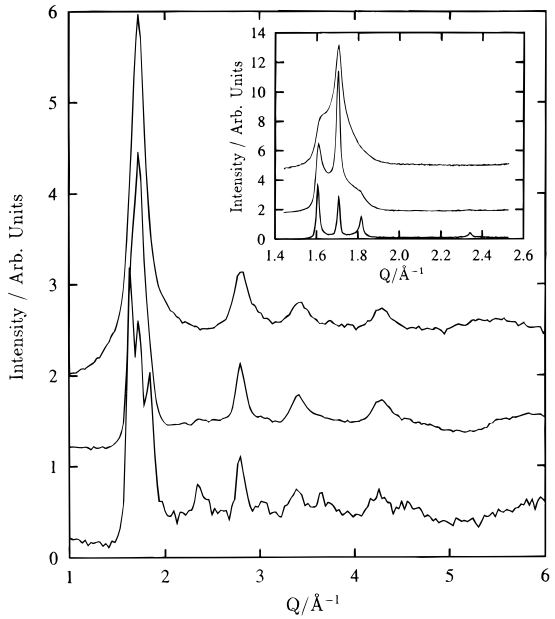

Figure 2. Diffraction patterns from ice in porous sol−gels. The upper plot is from D_2O in Aldrich 40 Å silica, $f = 1.0$, at −37 °C; middle plot, Unilever 200 Å, $f = 0.36$, −46 °C; lower plot, Unilever 500 Å, $f = 0.15$, −47 °C. For clarity these plots have been scaled to approximately the same peak intensity. The inset shows high-resolution measurements from these samples.

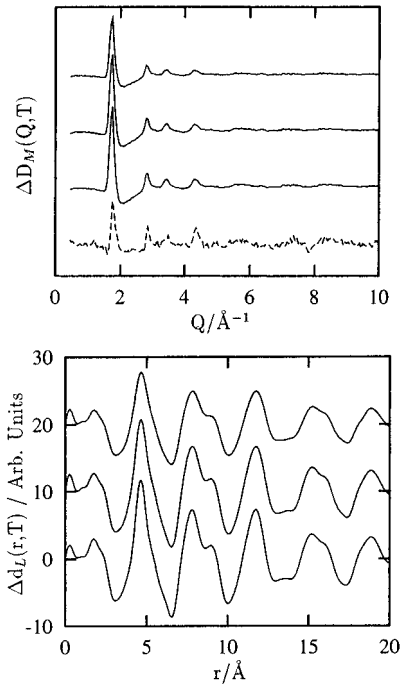

Figure 3. (a, top) Temperature difference functions from fully -filled Aldrich 60 Å silica. Solid lines are relative to $T_0 = 25$ °C, upper line is for $T = -17$ °C, middle $T = -50$ °C, and lower $T = -100$ °C. The broken line is for $T = -100$ °C relative to $T_0 = -50$ °C. (b, bottom) Fourier transformation of the $\Delta D_M(Q,T)$ functions (relative to $T_0 = 25$ °C) from part a. Upper line is for $T = -17$ °C, middle $T = -50$ °C, lower $T = -100$ °C.

of ice Ic. The peak at 2.34 $Å^{-1}$, which is a defining feature of ice Ih, is visible for the ice pattern from 500 Å pores, but absent for the two silicas of lower pore size despite the appearance of the peak at 1.61 $Å^{-1}$ in the patterns.

The asymmetric peak shape is characteristic of scattering from a two-dimensional crystal and resembles the Warren profile observed in graphite structures. This behavior has been used in a treatment by Elarby-Aouizerat *et al.*[9,10] of the cubic ice growth from quenched aqueous LiCl glasses, where it is proposed that the asymmetry of the ice Ic peaks gives rise to ice Ih-like defects occurring within ice Ic, possibly as stacking faults. The high Q-resolution of the G61 experiments enables this conjecture to be tested quantitatively, but it is found[11] that the peak cannot be simply represented by the Warren formalism.[12] The results therefore indicate either the presence of some anisotropic crystallite features or alternatively a form of disorder arising from defects in the lattice planes.

4.2. Temperature Variation Studies in 60 Å Pores. The diffraction pattern for D_2O water in filled pores of 60 Å Aldrich silica has been measured on the 7C2 diffractometer for the liquid phase (25 °C), the onset of nucleation (−17 °C), and lower temperatures (−50 and −100 °C). Using the liquid phase as a reference, the $\Delta D_M(Q,T)$ function has been evaluated for three ice phases and is shown in Figure 3a. The growth of the cubic ice pattern from the broad peaks of the water pattern is clearly observed and similar in shape to earlier work.[3,7] The overall shape remains identical for all temperatures, but the intensity increases with the change from −17 to −50 °C, indicating an evolution in the crystalline nature of the confined ice. Even for the change from −50 to −100 °C there is a small but systematic change in the diffraction pattern, as revealed by the direct difference function between these temperatures, which is also shown in Figure 3a.

The real-space changes are represented by the $\Delta d_L(r,T)$ function, evaluated from eq 6 and shown in Figure 3b. At short distances, there is an increase in correlations in the region of 2 Å which arises from the enhanced hydrogen-bonding of the ice phase compared to that of water. The prominent peak at 5 Å is a direct result of local tetrahedral-ordering of second and third nearest neighbor molecules and is also seen in the correlation function of amorphous ice.[13] Other features beyond 8 Å are due to the crystalline lattice, as the spatial correlations in water have decayed to negligible level at this distance. It is clear from Figure 3 that there is a systematic change with temperature that has a universal behavior for all pore systems based on the silica sol−gel material.

4.3. Ordered Mesoporous Aluminosilicates. The pore structure of the MCM-41 type aluminosilicates used in these experiments consists of an ordered matrix with a hexagonal lattice of uniaxial pores. The upper plots of Figure 4 show the patterns obtained on the G61 instrument for water/ice in the Al13 sample. The water supercooled (nucleating at ∼−20 °C) before "freezing" to give a pattern that cannot be ascribed to either ice Ic or Ih. The behavior is similar for the sample RJ31, but it was found necessary to cool to even lower temperatures to obtain any indication of a peak at 1.7 $Å^{-1}$. Figure 4 also shows the diffraction pattern from the liquid (at 25 °C) and water/ice (at −96 °C) confined in this sample. The lower curve of Figure 4 shows the difference function between −60 and −96 °C, emphasizing that the main structural change occurs below −60 °C. There is also an interesting difference in the behavior of the liquid and "solid" curves at lower Q-values. In general the liquid structure factor approaches a limiting value at $Q = 0$, which relates to the isothermal compressibility of the condensed phase and therefore gives some indication of the degree of fluidity. The change in intensity for this region (∼0.8−1.2 $Å^{-1}$) is small for the Al13 sample but is much more marked for the RJ31 sample. This difference in behavior suggests that the change in hydrophilicity of the surface, created by the increased number of hydroxyl groups, has a profound effect on the properties of the water/ice.

The state of the water/ice under these conditions seems paradoxical since the temperature is below the normal homo-

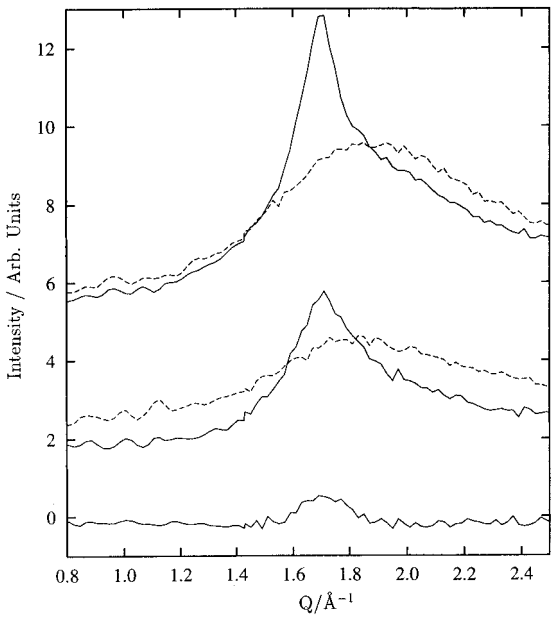

Figure 4. Diffraction patterns obtained from D_2O in two MCM-41 aluminosilicates ($f \approx 0.3$). The upper plots are from the Al13 sample at two temperatures, −14 °C (broken line) and −30 °C (solid line). The lower plots are from the RJ31 sample: broken line is for 25 °C, solid line is for −96 °C. The bottom plot is a temperature difference function for the RJ31 sample at −96 °C relative to −60 °C.

geneous nucleation temperature of −50 °C (for D_2O) and is therefore not expected to retain any liquid-like properties. Furthermore it is unlikely to be a glassy form of water due to a break in the continuity of state conditions between the supercooled liquid and the amorphous ice phases, such that a hyperquenched process is needed to produce the glassy form from micron-sized droplets of water. Low-density amorphous D_2O ice prepared by vapor deposition[13] does have a single sharp peak at 1.7 Å^{-1} so the data could indicate the presence of a glassy form, but this would be surprising in the context of other studies. Unfortunately, measurements of the full diffraction pattern for these samples have not yet been made, and the situation remains unclear until further studies are undertaken. It does, however, appear that this system is displaying the property of "frustrated nucleation".

5. Conclusions and Future Studies

The data presented in the previous sections provide a short survey of current work on the nucleation of ice in porous solids carried out by the UKC group and collaborators. There are a number of interesting conclusions and also some surprises indicating the complexity of the nucleation process. The first study based on the partial filling of variable pore sizes shows convincingly that the type of ice crystallites created is dependent on the geometrical characteristics of the liquid phase and the confining surface. The observation of hybrid patterns incorporating both cubic and hexagonal characteristics emphasizes the defective nature of the ice structure but has not yet been modeled in any realistic manner.

The temperature variation studies for the 60 Å pores indicate the universal behavior of the difference function for the sol−gel silica system. The puzzling feature is the continuing change of structure below −50 °C, which is small but significant. It is possible to speculate that the changes in the higher temperature regime arise from the gradual nucleation of supercooled water in highly constrained regions of the available volume between the silica walls and the ice interface. This effect could lead to increased local pressure, which causes a depression of the homogeneous nucleation point and therefore retains some water in a highly supercooled state below the −50 °C point. Another possibility is that the defective nature of the crystallites themselves causes disorder in the hydrogen-bonding network structure, leading to a partial delocalization of the deuterium positions in the lattice. The spatial correlations could be sensitive to variation in temperature over a wide range under these circumstances. Both of these explanations could be invoked to explain the structural behavior and would require alternative experimental investigation of the proton dynamics to resolve the remaining problems. It is already known from NMR studies that the proton mobility is anomalously high for ices formed in confined geometry, and it now seems that a combined study with the diffraction measurements could lead to a better understanding. Further neutron studies will also be undertaken to investigate the influences on the peak profile, the temperature dependence of the ices in different porous silicas, and also the "frustrated nucleation" in the mesoporous aluminosilicates by extending the temperature and Q-ranges.

Acknowledgment. One of us (J.M.B.) wishes to acknowledge the EPSRC for a studentship and the Barber Trust Fund for financial support to attend the "International Symposium on the Physics and Chemistry of Ice" conference in Hannover. Two of us (J.C.D. and P.B.) wish to acknowledge financial support from the British Council/DAAD for a travel grant in the ARC scheme. The experimental work was conducted at the Laboratoire Léon Brillouin in the Large Scale Facilities and the Human Capital Mobility programmes. Finally, but not lastly, we wish to thank Marie Claire Bellissent-Funel for invaluable assistance during the experimental work on the Orphée reactor and continuing collaboration on the topic of confined water.

References and Notes

(1) Steytler, D. C.; Dore, J. C.; Wright, C. J. *Mol. Phys.* **1983**, *48*, 1031; *J. Phys. Chem.* **1983**, *87*, 2458.
(2) Dunn, M.; Dore, J. C.; Chieux, P. *J. Cryst. Growth* **1988**, *92*, 233.
(3) Dore, J. C.; Coveney, F.; Bellissent-Funel, M.-C. *Recent Developments in the Physics of Fluids*; IOP Publishing Ltd.: Bristol, 1992; Chapter 4.
(4) Dore, J. C. *Molecular Liquids*; D. Reidel Publishing Co.: Dordrecht, 1984.
(5) Farman, H.; Coveney, F. M.; Dore, J. C. *Physica B* **1992**, *180*, 857.
(6) Dore, J. C.; Blakey, D. M. *J. Mol. Liq.* **1995**, *65*, 85.
(7) Motl, P.; Dore, J. C.; Bellissent-Funel, M.-C. *Hydrogen Bond Networks*; Kluwer Academic Publishers: Amsterdam, 1994; Chapter 4.
(8) Behrens, P.; Stucky, G. D. *Angew. Chem., Int. Ed. Engl.* **1993**, *32*, 696.
(9) Elarby-Aouizerat, A.; Jal, J.-F.; Dupuy, J.; Schildberg, H.; Chieux, P. *J. Phys. Colloq. C1* **1987**, *48*, 465.
(10) Elarby-Aouizerat, A.; Jal, J.-F.; Chieux, P.; Letoffé, J. M.; Claudy, P.; Dupuy, J. *J. Non-Cryst. Solids* **1988**, *104*, 203.
(11) Baker, J. M. Ph.D. thesis, University of Kent, 1997.
(12) Warren, B. E. *Phys. Rev.* **1941**, *59*, 693.
(13) Blakey, D. M. Ph.D. thesis, University of Kent, 1994.